International Geology Review
Publication details, including instructions for authors and subscription information:
http://www.tandfonline.com/loi/tigr20

Geochemical, Sr-Nd-Pb isotope, and zircon U-Pb geochronological constraints on the origin of Early Permian mafic dikes, northern North China Craton

Shen Liu[a], Caixia Feng[a], Bor-ming Jahn[b], Ruizhong Hu[c], Shan Gao[d], Ian M. Coulson[e], Guangying Feng[f], Shaocong Lai[a], Yuhong Yang[c] & Liang Tang[c]

[a] State Key Laboratory of Continental Dynamics and Department of Geology, Northwest University, Xi’an, 710069, PR China

[b] Department of Geosciences, National Taiwan University, Taipei, Taiwan

[c] State Key Laboratory of Ore Deposit Geochemistry, Institute of Geochemistry, Chinese Academy of Sciences, Guiyang, 550002, PR China

[d] State Key Laboratory of Geological Processes and Mineral Resources, China University of Geosciences, Wuhan, 430074, PR China

[e] Solid Earth Studies Laboratory, Department of Geology, University of Regina, Saskatchewan, CanadaS4S 0A2

[f] Institute of Geology, Chinese Academy of Geological Sciences, Beijing, 100037, PR China

Published online: 10 Apr 2013.

International Geology Review, 2013
Vol. 55, No. 13, 1626–1640, http://dx.doi.org/10.1080/00206814.2013.788242

Geochemical, Sr–Nd–Pb isotope, and zircon U–Pb geochronological constraints on the origin of Early Permian mafic dikes, northern North China Craton

Shen Liu[a]*, Caixia Feng[a], Bor-ming Jahn[b], Ruizhong Hu[c], Shan Gao[d], Ian M. Coulson[e], Guangying Feng[f], Shaocong Lai[a], Yuhong Yang[c] and Liang Tang[c]

[a]*State Key Laboratory of Continental Dynamics and Department of Geology, Northwest University, Xi'an 710069, PR China;* [b]*Department of Geosciences, National Taiwan University, Taipei, Taiwan;* [c]*State Key Laboratory of Ore Deposit Geochemistry, Institute of Geochemistry, Chinese Academy of Sciences, Guiyang 550002, PR China;* [d]*State Key Laboratory of Geological Processes and Mineral Resources, China University of Geosciences, Wuhan 430074, PR China;* [e]*Solid Earth Studies Laboratory, Department of Geology, University of Regina, Saskatchewan, Canada S4S 0A2;* [f]*Institute of Geology, Chinese Academy of Geological Sciences, Beijing 100037, PR China*

(*Accepted 18 March 2013*)

Dolerite dike swarms are widespread across the North China Craton (NCC) of Hebei Province (China) and Inner Mongolia. Here, we report new geochemical, Sr–Nd–Pb isotope, and U–Pb zircon ages for representative samples of these dikes. Laser ablation-inductively coupled plasma-mass spectrometry (LA-ICP-MS) U–Pb analysis yielded consistent Permian ages of 274.8 ± 2.9 and 275.0 ± 4.5 Ma for zircons extracted from two dikes. The dolerites have highly variable compositions (SiO_2 = 46.99–56.18 wt.%, TiO_2 = 1.27–2.39 wt.%, Al_2O_3 = 14.42–16.20 wt.%, MgO = 5.18–7.75 wt.%, Fe_2O_3 = 8.03–13.52 wt.%, CaO = 5.18–9.75 wt.%, Na_2O = 2.46–3.79 wt.%, K_2O = 0.26–2.35 wt.%, and P_2O_5 = 0.18–0.37 wt.%) and are light rare earth element (LREE) and large ion lithophile element (LILE, e.g. Rb, Ba, and K, and Pb in sample SXG1-9) enriched, and Th and high field strength element (HFSE, e.g. Nb and Ta in sample SXG1-9, and Ti) depleted. The mafic dikes have relatively uniform $(^{87}Sr/^{86}Sr)_i$ values from 0.7031 to 0.7048, $(^{206}Pb/^{204}Pb)_i$ from 17.77 to 17.976, $(^{207}Pb/^{204}Pb)_i$ from 15.50 to 15.52, $(^{208}Pb/^{204}Pb)_i$ from 37.95 to 38.03, and positive $\varepsilon_{Nd}(t)$ (3.6–7.3), and variable neodymium model ages (T_{DM1} = 0.75–0.99 Ga, T_{DM2} = 0.34–0.74 Ga). These data suggest that the dike magmas were derived from partial melting of a depleted region of the asthenospheric mantle, and that they fractionated olivine, pyroxene, plagioclase, K-feldspar, and Ti-bearing phases without undergoing significant crustal contamination. These mafic dikes within the NCC formed during a period of crustal thinning in response to extension after Permian collision between the NCC and the Siberian Block.

Keywords: Permian; mafic dikes; dolerite origin; northern NCC; Siberian Block

1. Introduction

Extensional belts within the continental lithosphere can provide important constraints on continental-scale crustal dynamics. Although a number of preliminary studies of orogenic belts within the North China Craton (NCC) and southern China have been undertaken, most have focussed solely on mantle–crust interaction during the Mesozoic and Precambrian (e.g. Chen and Shi 1983, 1994; Chen *et al.* 1992; Shao and Zhang 2002; Zhang and Sun 2002; Shao *et al.* 2003; Zhai *et al.* 2003, 2004; Xu 2004; Yang *et al.* 2004; Liu *et al.* 2005, 2006, 2008a, 2008b, 2009, 2012b, 2013; Peng *et al.* 2005, 2007, 2008, 2010, 2011a, 2011b; Hou *et al.* 2006; Wang *et al.* 2007; Hu *et al.* 2008; Lin *et al.* 2008; Wu *et al.* 2008; Zhu *et al.* 2008; Zhang 2009; John *et al.* 2010; Li *et al.* 2010; Peng 2010). In contrast, little research has focussed on Palaeozoic lithospheric extension in China, especially during the late Palaeozoic despite clear evidence of extensional tectonics in this part of Asia at this time.

Mafic dike swarms (e.g. lamprophyres, dolerites, and porphyritic dolerites) are thought to form during periods of lithospheric rifting (Hall 1982; Hall and Fahrig 1987; Tarney and Weaver 1987; Zhao and McCulloch 1993). These dikes are widespread throughout the NCC, and more than 600 dikes have been identified within swarms that trend NE–SW, NW–SE, and E–W (Liu *et al.* 2008a, 2008b, 2009, 2012a, 2012b, 2013). Studying the NCC mafic dikes provides information on processes involved in the generation of these widespread mafic magmas; in addition, investigating such dikes provides insight into lithospheric and tectonic processes, including extension, crust–lithosphere interaction, and magma sourcing during

*Corresponding author. Email: liushen@vip.gyig.ac.cn; liushen@nwu.edu.cn

Table 1. LA-ICP-MS U–Pb isotope data for zircons from mafic dikes of the NCC.

XFZ01	Isotopic				Ratios						Age (Ma)					
Spot	Th (ppm)	U (ppm)	Pb (ppm)	Th/U	$^{207}Pb/^{206}Pb$	1σ	$^{207}Pb/^{235}U$	1σ	$^{206}Pb/^{238}U$	1σ	$^{207}Pb/^{206}Pb$	1σ	$^{207}Pb/^{235}U$	1σ	$^{206}Pb/^{238}U$	1σ
1.1	442	522	34	0.85	0.0538	0.0016	0.3193	0.0204	0.0435	0.0006	363	46	289	8	275	4
2.1	228	418	642	0.55	0.0542	0.0018	0.3189	0.0206	0.0437	0.0006	379	48	289	8	276	4
3.1	578	613	85	0.94	0.0660	0.0036	0.3488	0.0199	0.0431	0.0007	807	79	333	15	276	4
4.1	1301	1432	355	0.91	0.0543	0.0016	0.3197	0.0205	0.0434	0.0007	384	43	289	8	274	4
5.1	563	884	61	0.64	0.0542	0.0017	0.3196	0.0207	0.0434	0.0006	379	48	289	8	274	4
6.1	855	1091	116	0.78	0.0543	0.0016	0.3194	0.0206	0.0435	0.0005	384	51	289	8	274	3
7.1	576	705	81	0.82	0.0545	0.0015	0.3193	0.0205	0.0435	0.0005	392	50	289	8	274	3
8.1	508	642	39	0.79	0.0543	0.0015	0.3196	0.0206	0.0433	0.0007	384	44	289	8	274	4
9.1	326	568	142	0.57	0.0544	0.0017	0.3196	0.0205	0.0436	0.0007	387	45	289	8	275	4
10.1	309	598	349	0.52	0.0545	0.0016	0.3191	0.0208	0.0434	0.0008	392	42	289	8	274	5
11.1	589	649	76	0.91	0.0546	0.0017	0.3194	0.0206	0.0438	0.0006	396	46	289	8	276	4
12.1	458	662	109	0.69	0.0544	0.0018	0.3195	0.0205	0.0435	0.0008	388	40	289	8	276	5
13.1	2282	3483	199	0.66	0.0547	0.00184	0.3194	0.0206	0.0432	0.0007	400	43	289	8	275	4
14.1	338	375	49	0.90	0.06091	0.00475	0.3136	0.03212	0.0433	0.0010	636	129	315	21	275	6
15.1	311	628	771	0.49	0.0661	0.0036	0.3485	0.0298	0.0432	0.0007	810	79	333	14	275	4
16.1	182	336	17.9	0.54	0.0608	0.0046	0.3334	0.0323	0.0435	0.0012	632	120	315	21	276	7
17.1	219	416	187	0.53	0.0664	0.0037	0.3486	0.0297	0.0434	0.00081	819	75	333	14	276	5
SXG01	Isotopic				Ratios						Age (Ma)					
Spot	Th (ppm)	U (ppm)	Pb (ppm)	Th/U	$^{207}Pb/^{206}Pb$	1σ	$^{207}Pb/^{235}U$	1σ	$^{206}Pb/^{238}U$	1σ	$^{207}Pb/^{206}Pb$	1σ	$^{207}Pb/^{235}U$	1σ	$^{206}Pb/^{238}U$	1σ
1.1	1310	1893	240	0.69	0.0463	0.0013	0.3136	0.0211	0.0435	0.0005	13	56	269	9	274	3
2.1	414	653	100	0.63	0.0461	0.0012	0.3135	0.0212	0.0434	0.0004	3	59	269	9	275	2
3.1	716	1277	135	0.56	0.0531	0.0023	0.3156	0.0213	0.0435	0.0005	333	59	286	9	274	3
4.1	532	923	101	0.58	0.0529	0.0023	0.3061	0.0212	0.0435	0.0005	325	55	287	9	274	3
5.1	592	926	123	0.64	0.0462	0.0013	0.3141	0.0213	0.0435	0.0005	8	56	270	9	274	3
6.1	555	996	106	0.56	0.0533	0.0024	0.3058	0.0213	0.0436	0.0006	342	54	286	9	275	4
7.1	622	1278	130	0.49	0.0528	0.0022	0.3148	0.0214	0.0432	0.0005	320	58	286	9	275	3
8.1	400	628	82	0.64	0.0461	0.0052	0.3149	0.0213	0.0439	0.0007		225	250	25	277	4
9.1	559	1161	114	0.48	0.0531	0.0022	0.3057	0.0214	0.0434	0.0006	333	52	286	9	274	4
10.1	1036	1537	180	0.67	0.0528	0.0021	0.3055	0.0213	0.0433	0.0006	320	54	286	9	275	4
11.1	642	1056	122	0.61	0.0534	0.0023	0.3153	0.0213	0.0436	0.0006	347	54	286	9	275	4
12.1	1147	1980	210	0.58	0.0541	0.0022	0.3149	0.0215	0.0434	0.0006	375	54	286	9	274	4
13.1	1138	1752	214	0.65	0.0533	0.0021	0.3154	0.0214	0.0434	0.0005	342	60	286	9	274	3
14.1	482	1151	107	0.42	0.0523	0.0023	0.3055	0.0217	0.0441	0.0006	299	57	286	9	278	4
15.1	874	1438	155	0.61	0.0532	0.0022	0.3148	0.0216	0.0435	0.0006	337	57	286	9	275	4

breakup of the NCC (e.g. Liu *et al.* 2005, 2006, 2008a, 2008b, 2009, 2012a, 2012b, 2013). Furthermore, the presence of significant mineralization within the NCC means that the relationship between ore formation and magmatic activity – even if magmatism was just a source of heat for mineralizing systems – is significant, and can be illuminated by studying these mafic dike swarms.

The fact that these key pieces of information are currently lacking means that an investigation of the geochronological, geochemical, and isotopic characteristics of the late Palaeozoic mantle lithosphere associated with the NCC is required. Our investigation responds to this need by examining mafic dikes. Here, we present new laser ablation inductively coupled plasma mass spectrometry (LA-ICP-MS) zircon U–Pb, petrological, whole-rock geochemical, and Sr–Nd–Pb isotopic data for representative samples from a swarm in the northern NCC. These data allow us to constrain the emplacement ages and petrogenesis of these mafic dikes.

2. Geological setting and petrography

The NCC consists of Archaean eastern and western blocks, and an NS-trending Proterozoic mid-continental orogenic belt (Zhao *et al.* 2001). The two study areas that form the focus of this paper are located in the Pinquan area of north Hebei Province (XFZ1-13) and the Chifeng area of Inner Mongolia (SXG1-9), both within the northern NCC. Dolerite dikes from these areas were sampled during this study (Table 1; Figures 1B and 1C); these dikes were intruded into areas dominated by granites of unknown age, volcanics, and Jurassic sediments (Figures 1B and 1C), and the dikes cross-cut all of these lithologies. Individual dikes are vertical, trend NE–SW to NW–SE, are 0.2–2.0 km wide, and 2.0–8.0 km long (Figures 1B and 1C). Representative photomicrographs of mafic dike lithologies from the Xinfangzi (samples XFZ 2 and 5) and Shangxigou (samples SXG 1 and 3) areas are shown in Figure 2. The dikes are all dolerites and have typical dolerite/diabase textures. Dolerites in the Xinfangzi area contain 33–36 modal% medium-grained clinopyroxene (2.3–4.5 mm) and lath-shaped plagioclase (1.6–3.0 mm) phenocrysts in a 65–70 modal% groundmass of clinopyroxene (0.04–0.06 mm), plagioclase (0.03–0.06 mm), and minor magnetite (~0.04 mm). In contrast, dolerite dikes in the Shangxigou area contain 32–35 modal% medium- to coarse-grained clinopyroxene (2.2–4.3 mm) and plagioclase (1.5–3.0 mm) phenocrysts within a 65–70 modal% matrix of clinopyroxene (0.04–0.07 mm), plagioclase (0.03–0.05 mm), minor magnetite (0.04–0.06 mm), and chlorite.

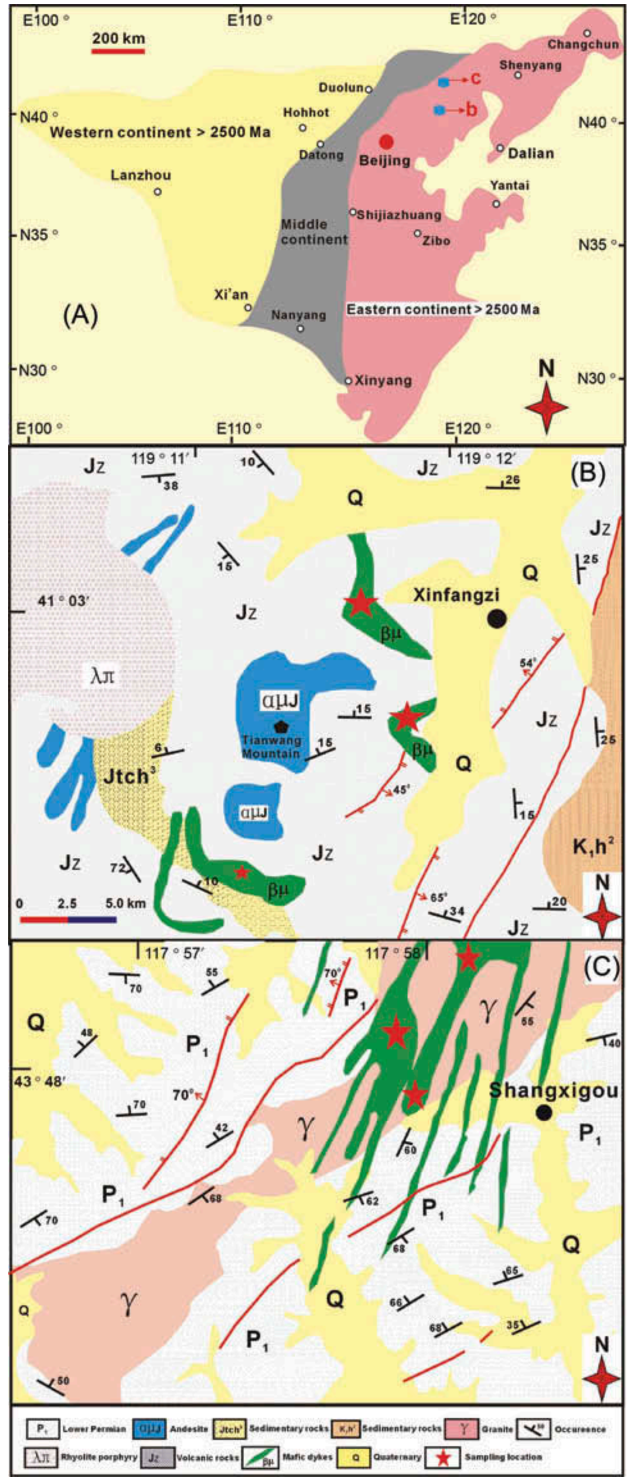

Figure 1 (A). Study areas in China. (B) and (C) Geological maps of the two study areas, showing the distribution of mafic dikes and sampling localities.

3. Analytical techniques

3.1 *Zircon LA-ICP-MS U–Pb dating*

Zircon was separated from two samples (XFZ01 and SXG01) using conventional heavy liquid and magnetic techniques at the Langfang Regional Geological Survey, Hebei Province, China. After separation and mounting, the internal and external structures of zircons were imaged using transmitted and reflected light, and by cathodoluminescence (CL) at the State Key Laboratory

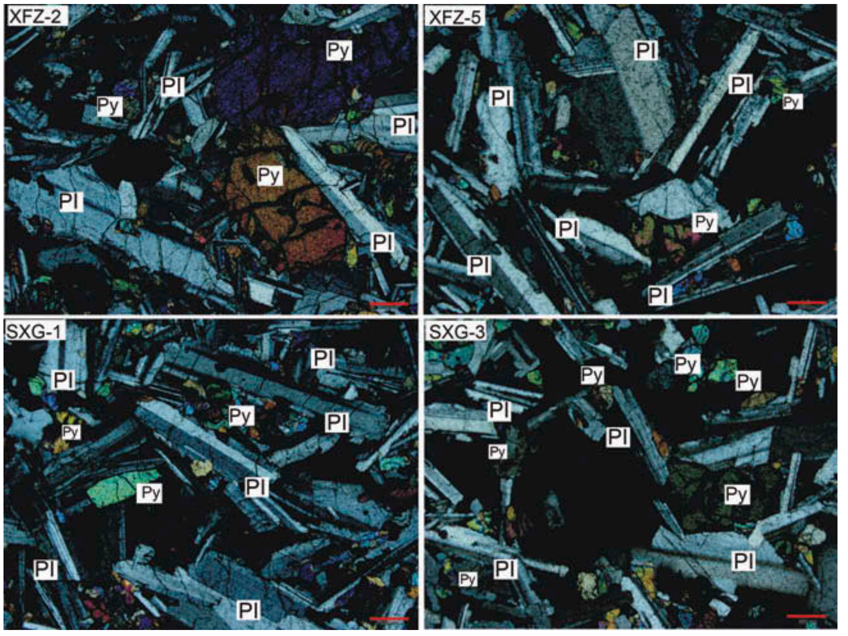

Figure 2. Representative photomicrographs illustrating the petrography of mafic dikes from the northern NCC, China; all samples have doleritic textures and hence are termed dolerite dikes.
Note: Py = pyroxene, Pl = plagioclase.

of Continental Dynamics, Northwest University, China. Prior to zircon U–Pb dating, grain mount surfaces were washed in dilute HNO_3 and pure alcohol to remove any potential lead contamination. Zircon U–Pb ages were determined using LA-ICP-MS (Table 1; Figure 3) and an Agilent 7500a ICP-MS instrument equipped with a 193 nm excimer laser at the State Key Laboratory of Geological Processes and Mineral Resources, China University of Geoscience, Wuhan, China. A Zircon #91500 standard was used for quality control, and a NIST 610 standard was used for data optimization. A spot diameter of 24 μm was used during analysis, employing the methodology described by Yuan *et al.* (2004) and Liu *et al.* (2010). Common Pb correction was undertaken following Andersen (2002), and the resulting data were processed using the GLITTER and ISOPLOT programs (Ludwig 2003; Table 1; Figure 3). Uncertainties on individual LA-ICP-MS analyses are quoted at the 95% (1σ) confidence level.

3.2 Whole-rock geochemistry

The whole-rock and Sr–Nd–Pb isotope geochemical compositions of 22 samples were determined during this study. Prior to whole-rock geochemical analysis, samples were trimmed to remove altered surfaces, cleaned with de-ionized water, and then crushed and powdered in an agate mill. Major element concentrations were determined on fused glass discs using a PANalytical Axios-advance (Axios PW4400) X-ray fluorescence spectrometer (XRF) at the State Key Laboratory of Ore Deposit Geochemistry, Institute of Geochemistry, Chinese Academy of Sciences, Guiyang, China. These analyses have a precision of <5%, as determined using GSR-1 and GSR-3 Chinese National standards (Table 2). Loss on ignition (LOI) values were obtained using 1 g of powder heated to 1100°C for 1 hour. Trace element concentrations were determined using ICP-optical emission spectrometry (OES) and ICP-MS at the National Research Centre of Geo-analysis, Chinese Academy of Geosciences, Guiyang, China, using the procedures outlined in Qi *et al.* (2000). Triplicate analyses were reproducible to within 5% for all elements, and analysis of the OU-6 and GBPG-1 international standards agreed with recommended values (Table 3).

3.3 Sr–Nd–Pb isotope analyses

Sample powders used for Rb–Sr and Sm–Nd isotope analysis were spiked with mixed isotope tracers, dissolved in Teflon capsules with HF and HNO_3 acids, and separated by conventional cation-exchange techniques. Isotopic measurements were performed using a Finnigan Triton Ti thermal ionization mass spectrometer at the State Key Laboratory of Geological Processes and Mineral Resources, China University of Geosciences, Wuhan, China. Procedural blanks yielded concentrations of <200 pg for Sm and Nd, and <500 pg for Rb and Sr. Mass fractionation corrections for Sr and Nd isotopic ratios were based on $^{86}Sr/^{88}Sr = 0.1194$ and $^{146}Nd/^{144}Nd = 0.7219$, respectively, and analysis of the NBS987 and La Jolla

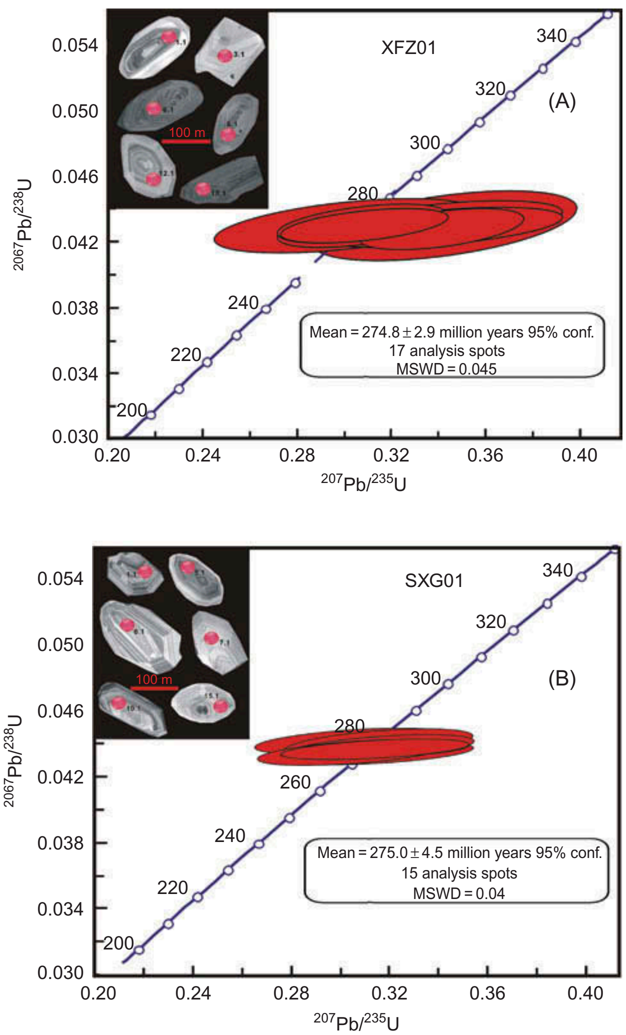

Figure 3. Zircon LA-ICP-MS U–Pb concordia diagrams and CL images of zircons separated from mafic dike samples from the northern NCC, China.

standards yielded values of $^{87}Sr/^{86}Sr = 0.710246 \pm 16$ (2σ) and $^{143}Nd/^{144}Nd = 0.511863 \pm 8$ (2σ), respectively. Pb was separated and purified by conventional cation-exchange techniques (AG1 × 8, 200–400 resin) using diluted HBr as an eluent, yielding procedural blanks with Pb concentrations of <50 pg. Repeat analysis of the NBS981 standard during Pb isotope determinations yielded values of $^{204}Pb/^{206}Pb = 0.0896 \pm 15$, $^{207}Pb/^{206}Pb = 0.9145 \pm 8$, and $^{208}Pb/^{206}Pb = 2.162 \pm 2$. Total procedural Pb blanks yielded Pb values of 0.1–0.3 ng, and Sr–Nd–Pb isotope data are presented in Tables 4 and 5.

4. Results

4.1 Zircon U–Pb ages

Euhedral zircons in samples XFZ01 and SXG01 are clean and prismatic, and have oscillatory magmatic zoning (Figure 3). Seventeen zircons from sample XFZ01 yielded a weighted mean $^{206}Pb/^{238}U$ age of 274.8 ± 2.9 Ma (1σ, 95% confidence interval; Table 1; Figure 3A), with 15 zircons from sample SXG01 yielding a weighted mean $^{206}Pb/^{238}U$ age of 275.0 ± 4.5 Ma (1σ; 95% confidence interval; Table 1; Figure 3B). These new data provide the best estimates of mafic dike crystallization ages in the Xinfangzi and Shangxigou areas, and no inherited zircons were observed in either sample population.

4.2 Major and trace element geochemistry

The whole-rock geochemical compositions of the mafic dikes sampled during this study are listed in Tables 2 and 3.

The mafic dikes have a wide range of compositions, with $SiO_2 = 46.99$–56.18 wt.%, $TiO_2 = 1.27$–2.39 wt.%, $Al_2O_3 = 14.42$–16.20 wt.%, $MgO = 5.18$–7.75 wt.%, $Fe_2O_3 = 8.03$–13.52 wt.%, $CaO = 5.18$–9.75 wt.%, $Na_2O = 2.46$–3.79 wt.%, $K_2O = 0.26$–2.35 wt.%, and $P_2O_5 = 0.18$–0.37 wt.%. All of these mafic dikes plot close to the alkaline–sub-alkaline field boundary on a total alkali-silica (TAS) diagram (Figure 4A); these dikes also straddle the join between shoshonitic and calc-alkaline series in a Na_2O *versus* K_2O diagram (Figure 4B). These mafic dikes have negative correlations between SiO_2, TiO_2, Fe_2O_3, and P_2O_5 concentrations and MgO (Figures 5A, 5B, 5D, and 5H), and are light rare earth element (LREE)-enriched and heavy rare earth element (HREE)-depleted, with a wide range in $(La/Yb)_N$ (1.7–8.9) and Eu/Eu* (0.6–0.9) values (Table 3; Figure 6A). In addition, mafic dikes from the Xinfangzi have much steeper REE trends (Figure 6A), with significant LREE-enrichments and HREE-depletions; these dikes contrast significantly with dikes from the Shangxigou area, which have a concave upwards pattern that indicates LREE-enrichment but not significant HREE-depletion. Dike samples from both areas are large ion lithophile element (LILE)-enriched (e.g. Pb in sample SXG1-9, along with Rb, Ba, and K in other samples), and Th-, Ti-, and occasionally Nb–Ta-depleted in primitive mantle-normalized trace element diagrams (Figure 6B).

4.3 Sr–Nd and Pb isotopes

The Sr–Nd isotopic compositions of eight representative dikes from both field areas were determined during this study (Table 4). These mafic dikes have a wide range of $(^{87}Sr/^{86}Sr)_i$ (0.7031–0.7048) and $\varepsilon_{Nd}(t)$ (3.6–7.3) values, suggesting they formed from magmas generated from a depleted mantle source. These Sr–Nd isotope compositions are not comparable to other late Palaeozoic mafic rocks within Inner Mongolia (Wu *et al.* 2007; Miao *et al.* 2008; Chen *et al.* 2012; Figure 7), but are similar to MORB compositions. The mafic dikes have $(^{206}Pb/^{204}Pb)_i$, $(^{207}Pb/^{204}Pb)_i$, and $(^{208}Pb/^{204}Pb)_i$ values

Table 2. Major element concentrations (in wt.%) for mafic dikes of the NCC; LOI = loss on ignition, $Mg^{\#} = 100 \times Mg/(Mg + Fe)$ in atomic proportions, RV* = recommended values, MV* = measured values; values for GSR-1 and GSR-3 are from Wang *et al.* (2003).

Sample	SiO_2	TiO_2	Al_2O_3	Fe_2O_3	MnO	MgO	CaO	Na_2O	K_2O	P_2O_5	LOI	Total	$Mg^{\#}$
XFZ-1	50.83	2.29	14.70	12.60	0.15	5.21	8.13	3.79	1.06	0.34	0.73	99.82	48
XFZ-2	50.85	2.15	14.90	12.41	0.15	5.28	8.10	3.65	1.07	0.33	0.24	99.12	48
XFZ-3	50.22	2.23	14.70	12.36	0.15	5.22	8.15	3.62	1.06	0.33	1.40	99.45	48
XFZ-4	50.40	2.21	14.74	12.43	0.15	5.28	8.11	3.66	1.08	0.33	0.79	99.19	48
XFZ-5	51.01	2.18	14.98	12.52	0.15	5.31	8.25	3.73	1.08	0.33	0.56	100.11	48
XFZ-6	51.30	2.21	15.08	12.66	0.15	5.44	8.34	3.62	1.10	0.33	0.50	100.71	49
XFZ-7	50.01	2.21	13.99	13.52	0.16	6.02	7.97	3.48	1.07	0.33	0.51	99.27	49
XFZ-8	50.73	2.18	14.84	12.70	0.15	5.46	8.27	3.55	1.07	0.33	0.79	100.08	49
XFZ-9	51.78	2.32	14.60	12.74	0.15	5.35	8.08	3.25	1.15	0.37	0.88	100.66	48
XFZ-10	50.80	2.19	14.57	12.29	0.15	5.37	7.98	3.15	1.28	0.36	1.14	99.26	49
XFZ-11	50.89	2.29	14.42	12.29	0.15	5.22	8.10	3.02	1.24	0.37	1.14	99.13	48
XFZ-12	51.26	2.27	14.49	12.30	0.14	5.18	7.99	3.10	1.32	0.37	1.26	99.69	48
XFZ-13	51.03	2.25	14.44	12.92	0.15	5.66	8.08	3.09	1.21	0.35	0.87	100.06	49
SXG-1	48.45	1.54	16.21	10.94	0.18	6.79	9.75	2.46	0.33	0.24	3.23	100.11	58
SXG-2	47.19	1.91	16.20	11.38	0.20	7.63	7.68	2.74	1.88	0.28	3.25	100.33	60
SXG-3	50.80	1.60	15.03	11.16	0.19	5.83	7.46	3.52	1.44	0.24	2.88	100.16	53
SXG-4	54.61	1.27	15.01	8.23	0.14	5.54	5.18	3.31	2.35	0.18	3.97	99.80	60
SXG-5	49.37	1.33	15.50	10.13	0.15	7.75	9.30	2.46	0.26	0.18	3.36	99.78	63
SXG-6	48.41	2.02	15.71	11.95	0.18	6.42	9.08	2.96	0.62	0.31	2.28	99.95	54
SXG-7	46.99	1.94	15.70	10.89	0.18	7.22	7.25	3.32	1.20	0.29	4.56	99.53	59
SXG-8	52.38	1.66	14.88	10.46	0.18	5.98	7.12	3.20	1.56	0.26	3.15	100.83	56
SXG-9	56.18	1.27	14.89	8.03	0.13	5.49	5.39	3.03	2.35	0.19	2.79	99.74	60
GSR-3 (RV*)	44.64	2.37	13.83	13.4	0.17	7.77	8.81	3.38	2.32	0.95	2.24	99.88	
GSR-3 (MV*)	44.75	2.36	14.14	13.35	0.16	7.74	8.82	3.18	2.3	0.97	2.12	99.89	
GSR-1(RV*)	72.83	0.29	13.4	2.14	0.06	0.42	1.55	3.13	5.01	0.09	0.7	99.62	
GSR-1 (MV*)	72.65	0.29	13.52	2.18	0.06	0.46	1.56	3.15	5.03	0.11	0.69	99.70	

of 17.91–17.83, 15.50–15.52, and 37.95–38.03, respectively, similar to the isotopic compositions of Permian basalts from Inner Mongolia, China (Chen *et al.* 2012; Figures 8A and 8B), and they plot in the I-MORB compositional field (Figure 8A).

5. Genesis of mafic dike magmas

5.1 Mantle source

With the exception of three samples (SXG-4, 8, and 9), the mafic dikes contain low concentrations of SiO_2 (46.99–52.0 wt.%; Table 2), suggesting that the magmas that formed these rocks were derived from an ultramafic (i.e. mantle) source, and not by melting of crustal material. An ultramafic source is also supported by the relatively high MgO (5.18–7.75 wt.%), Ni, and Cr concentrations within these rocks, and the elevated $Mg^{\#}$ values (48–60) of mafic dikes from the Xinfangzi and Shangxigou areas. Crustal rocks are likely to be a potential source for these mafic magmas, as partial melting of any crustal material (e.g. Hirajima *et al.* 1990; Zhang *et al.* 1995; Kato *et al.* 1997) or lower crustal intermediate granulites in the deep crust (Gao *et al.* 1998a, 1998b) would produce high-Si, low-Mg melts (i.e. granitoid liquids). Mafic dikes in the study area have low initial $^{87}Sr/^{86}Sr$ ratios (0.7031–0.7048) and positive but variable $\varepsilon_{Nd}(t)$ values (3.6–7.3; Tables 4 and 5), consistent with derivation from a depleted lithospheric mantle source or from the asthenospheric mantle. It is generally accepted that the lithospheric mantle has enriched initial $^{87}Sr/^{86}Sr$ ratios and typically low $\varepsilon_{Nd}(t)$ values (Zhang *et al.* 2005), whereas magmas sourced from the asthenospheric mantle are characterized by depleted compositions with low $(^{87}Sr/^{86}Sr)_i$ and high $\varepsilon_{Nd}(t)$ values (Saunders *et al.* 1992). This suggests that the NCC mafic dikes studied here formed from magmas sourced from the asthenospheric mantle, a hypothesis that is further supported by the Pb isotope compositions of these dikes (Table 5; Figures 8A and 8B).

5.2 Crustal contamination

Crustal contamination can lead to significant Sr–Nd isotope enrichments in basaltic rocks. The fact that the dolerites studied here are characterized by depleted Sr isotopic compositions and positive $\varepsilon_{Nd}(t)$ values suggests that the magmas that formed these dikes did not assimilate significant crustal material. In addition, crustal contamination would cause significant variation in Sr–Nd isotope compositions, positive correlations between MgO and $\varepsilon_{Nd}(t)$ values (3.6–7.3), and negative correlations between MgO and $(^{87}Sr/^{86}Sr)_i$ ratios (0.7031–0.7048), features that are absent from the dolerite samples analysed during this study (Figures 7 and 9).

Table 3. Trace element compositions (in ppm) of mafic dikes within the NCC; values for GBPG-1 and OU-6 are from Thompson *et al.* (2000) and Potts and Kane (2005), respectively.

Sample	XFZ-1	XFZ-2	XFZ-3	XFZ-4	XFZ-5	XFZ-6	XFZ-7	XFZ-8	XFZ-9	XFZ-10	XFZ-11	XFZ-12	XFZ-13	SXG-1	SXG-2	SXG-3	SXG-4	SXG-5	SXG-6	SXG-7	SXG-8	SXG-9	OU-6 (RV*)	OU-6 (MV*)	GBPG-1 (RV*)	GBPG-1 (MV*)
V	216	202	213	206	206	203	212	205	221	213	219	206	217	240	252	251	170	200	253	248	201	165	129	131	96.5	103
Cr	104	109	114	109	102	99.7	104	99.7	98.2	96.8	97.0	94.3	100	290	277	227	244	345	234	278	211	261	70.8	73.5	181	187
Ni	111	106	127	101	96.4	92.2	110	88.9	71.6	76.2	72.8	70.0	81.2	50.7	121	68.5	101	148	63.0	118	92.8	223	39.8	42.5	59.6	60.6
Rb	20.2	15.0	17.2	20.1	17.2	19.0	19.7	20.2	22.8	25.9	29.6	29.1	23.6	15.6	71.4	46.2	60.1	8.01	22.1	45.9	50.5	65.3	120	122	56.2	61.4
Sr	448	440	462	450	451	453	436	456	445	451	465	428	459	202	334	298	314	192	273	317	279	303	131	136	364	377
Y	24.6	22.7	24.7	23.6	23.6	23.2	24.5	23.3	24.3	23.9	24.7	23.2	23.7	30.0	32.5	32.0	33.5	28.1	34.9	33.1	32.4	35.2	27.4	26.2	18.0	17.2
Zr	193	179	190	188	184	182	187	183	186	183	190	180	180	133	153	138	188	133	161	156	138	196	174	183	232	224
Nb	27.6	25.7	27.0	26.3	26.1	25.5	26.7	25.8	30.2	29.2	30.5	28.6	29.3	4.29	4.35	4.62	5.27	3.55	5.68	4.26	5.21	6.57	14.8	15.3	9.93	8.74
Ba	289	273	294	292	283	283	295	280	281	283	288	273	281	132	620	344	914	111	162	407	361	623	477	486	908	921
La	22.8	21.5	23.1	22.0	22.2	21.9	23.0	21.7	22.0	21.9	22.0	21.3	21.7	8.76	8.19	11.2	15.0	8.65	10.3	8.25	11.6	15.9	33.0	33	53.0	51
Ce	46.1	43.4	45.9	45.3	44.2	44.3	45.8	44.0	42.7	42.8	43.1	41.5	42.4	22.3	22.7	27.2	34.9	21.6	26.6	22.5	26.9	35.0	74.4	78	103	105
Pr	5.77	5.41	5.76	5.57	5.54	5.45	5.76	5.54	5.51	5.45	5.57	5.35	5.44	3.35	3.51	3.99	4.78	3.24	4.03	3.56	3.79	4.73	7.80	8.1	11.5	11.6
Nd	24.6	22.8	23.9	23.6	23.3	23.0	23.7	23.1	22.8	22.6	23.3	22.1	22.8	15.7	17.4	17.4	20.5	14.8	19.3	17.5	16.9	19.3	29.0	30.6	43.3	42.4
Sm	6.00	5.39	5.78	5.65	5.65	5.69	5.87	5.67	5.54	5.45	5.77	5.20	5.60	4.22	4.82	4.72	5.22	4.10	5.02	5.03	4.49	4.89	5.92	5.99	6.79	6.63
Eu	2.00	1.89	2.03	1.96	1.96	1.91	2.04	1.93	1.88	1.84	1.96	1.80	1.89	1.47	1.74	1.51	1.34	1.25	1.81	1.68	1.45	1.31	1.36	1.35	1.79	1.69
Gd	5.34	4.81	5.39	5.13	5.14	4.95	5.32	5.05	4.94	4.96	5.13	4.88	4.86	4.13	4.80	4.54	5.16	3.81	5.06	4.85	4.47	4.85	5.27	5.50	4.74	4.47
Tb	0.95	0.90	0.92	0.89	0.88	0.92	0.95	0.88	0.92	0.94	0.98	0.90	0.91	0.88	0.98	0.95	1.00	0.82	1.06	0.97	0.93	0.97	0.85	0.83	0.60	0.59
Dy	5.02	4.67	5.04	4.94	4.80	4.79	5.06	4.77	4.71	4.81	4.99	4.51	4.74	5.36	5.82	5.50	5.96	5.13	6.33	6.01	5.53	5.84	4.99	5.06	3.26	3.17
Ho	1.01	0.94	0.97	0.96	0.95	0.98	1.00	0.96	0.98	0.97	0.98	0.91	0.95	1.24	1.29	1.27	1.35	1.12	1.39	1.31	1.28	1.34	1.01	1.02	0.69	0.66
Er	2.31	2.19	2.33	2.22	2.23	2.21	2.37	2.34	2.28	2.33	2.31	2.18	2.24	3.31	3.46	3.40	3.69	3.08	3.68	3.42	3.40	3.63	2.98	3.07	2.01	2.02
Tm	0.30	0.29	0.29	0.29	0.29	0.29	0.31	0.30	0.29	0.30	0.29	0.27	0.29	0.49	0.50	0.50	0.51	0.46	0.54	0.51	0.49	0.53	0.44	0.45	0.30	0.29
Yb	1.74	1.70	1.79	1.75	1.68	1.69	1.84	1.75	1.72	1.73	1.68	1.61	1.74	3.07	3.24	3.29	3.54	2.88	3.39	3.22	3.15	3.47	3.00	3.09	2.03	2.03
Lu	0.24	0.24	0.24	0.24	0.24	0.24	0.27	0.24	0.23	0.24	0.23	0.23	0.24	0.46	0.47	0.49	0.50	0.43	0.52	0.49	0.47	0.52	0.45	0.47	0.31	0.31
Hf	4.63	4.49	4.64	4.44	4.44	4.41	4.54	4.47	4.38	4.40	4.50	4.34	4.28	3.32	3.71	3.58	4.92	3.38	3.90	3.80	3.59	5.10	4.70	4.86	6.07	5.93
Ta	1.63	1.56	1.61	1.59	1.52	1.53	1.60	1.51	1.56	1.59	1.58	1.56	1.60	0.29	0.28	0.32	0.37	0.24	0.37	0.28	0.35	0.53	1.06	1.02	0.40	0.46
Pb	3.66	2.92	2.94	3.01	2.83	2.98	3.08	2.80	2.53	2.60	2.61	2.94	2.49	5.74	5.89	5.68	9.51	4.27	3.14	5.32	4.81	4.44	28.2	32.7	14.1	14.5
Th	2.54	2.42	2.50	2.48	2.51	2.41	2.57	2.42	2.50	2.49	2.55	2.41	2.46	0.93	0.58	2.30	4.01	1.43	0.99	0.53	2.36	4.33	11.5	13.9	11.2	11.4
U	0.63	0.61	0.62	0.60	0.61	0.60	0.62	0.61	0.73	0.64	0.66	0.65	0.64	0.29	0.19	0.83	1.23	0.46	0.32	0.22	0.78	1.30	1.96	2.19	0.90	0.99
$(La/Yb)_N$	8.9	8.5	8.7	8.5	8.9	8.7	8.5	8.4	8.6	8.6	8.8	8.9	8.5	1.9	1.7	2.3	2.9	2.0	2.1	1.7	2.5	3.1				
δEu	0.8	0.8	0.8	0.8	0.8	0.8	0.8	0.8	0.8	0.8	0.8	0.8	0.8	0.8	0.9	0.8	0.6	0.7	0.9	0.8	0.8	0.6				

Note: RV* = recommended values and MV* = measured values.

Table 4. Sr–Nd isotopic compositions of mafic dikes within the northern NCC, using Chondrite Uniform Reservoir (CHUR) values, and decay constants of $\lambda_{Rb} = 1.42 \times 10^{-11}$ year^{-1} (Steiger and Jäger 1977) and $\lambda_{Sm} = 6.54 \times 10^{-12}$ year^{-1} (Lugmair and Harti 1978).

Sample	Sm (ppm)	Nd (ppm)	Rb (ppm)	Sr (ppm)	$^{87}Rb/^{86}Sr$	$^{87}Sr/^{86}Sr$	2σ	$(^{87}Sr/^{86}Sr)_i$	$^{147}Sm/^{144}Nd$	$^{143}Nd/^{144}Nd$	2σ	$(^{143}Nd/^{144}Nd)_i$	$\varepsilon_{Nd}(t)$	T_{DM1}(Ga)	T_{DM2}(Ga)
XFZ-1	6.00	24.6	20.2	448	0.1307	0.704749	10	0.704239	0.1473	0.512732	8	0.512468	3.6	0.96	0.74
XFZ-3	5.78	23.9	17.2	462	0.1073	0.704896	12	0.704477	0.1462	0.512736	9	0.512473	3.7	0.94	0.73
XFZ-5	5.65	23.3	17.2	451	0.1100	0.704815	10	0.704385	0.1464	0.512737	9	0.512473	3.7	0.94	0.73
XFZ-8	5.67	23.1	20.2	456	0.1279	0.704813	8	0.704313	0.1484	0.512736	10	0.512469	3.6	0.97	0.74
XFZ-10	5.45	22.6	25.9	451	0.1657	0.704796	12	0.704149	0.1459	0.512733	9	0.512471	3.6	0.94	0.74
SXG-2	4.82	17.4	71.4	334	0.6175	0.706365	10	0.703951	0.1677	0.512952	8	0.512650	7.1	0.99	0.38
SXG-3	4.72	17.4	46.2	298	0.4482	0.705207	12	0.703597	0.0938	0.512844	9	0.512689	7.3	0.75	0.34
SXG-8	4.49	16.9	50.5	279	0.5244	0.705004	10	0.703120	0.1097	0.512856	10	0.512675	7.1	0.85	0.36

Table 5. Pb isotope compositions of mafic dikes from the northern NCC.

Sample	U (ppm)	Pb (ppm)	Th (ppm)	$^{238}U/^{204}Pb$	$^{235}U/^{204}Pb$	$^{232}Th/^{204}Pb$	$^{206}Pb/^{204}Pb$	$^{207}Pb/^{204}Pb$	$^{208}Pb/^{204}Pb$	$(^{206}Pb/^{204}Pb)i$	$(^{207}Pb/^{204}Pb)_i$	$(^{208}Pb/^{204}Pb)i$
XFZ-1	0.53	2.33	0.59	14.385	0.104	16.547	18.456	15.545	38.177	17.829	15.513	37.950
XFZ-3	0.56	2.26	0.56	15.668	0.114	16.190	18.452	15.543	38.176	17.769	15.508	37.954
XFZ-5	0.49	2.18	0.54	14.212	0.103	16.184	18.453	15.541	38.175	17.834	15.509	37.954
SXG-2	0.51	1.88	0.64	17.241	0.125	22.357	18.671	15.542	38.332	17.920	15.503	38.025
SXG-3	0.54	1.95	0.66	17.601	0.128	22.229	18.674	15.543	38.333	17.907	15.503	38.028
SXG-8	0.38	1.47	0.35	16.401	0.119	15.610	18.682	15.554	38.185	17.967	15.517	37.971

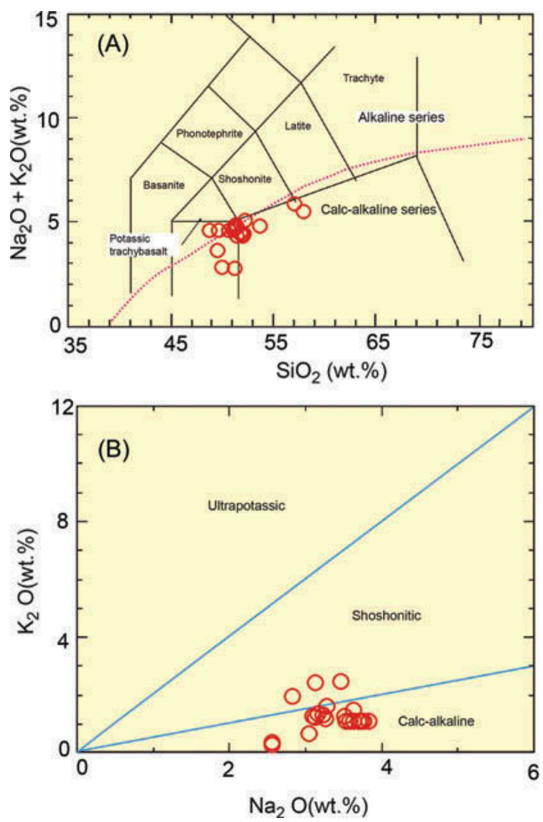

Figure 4. Classification of mafic dikes from the NCC by (A) TAS (after Middlemost 1994; Le Maitre 2002), where all major element concentrations are recalculated to 100% volatile-free compositions, and (B) K_2O *versus* Na_2O.

In addition, the absence of any inherited zircons suggests that the magmas that formed the dikes in the study area underwent negligible crustal contamination. In summary, the geochemical and isotopic signatures of the dolerites are indicative of derivation from a depleted asthenospheric mantle source.

5.3 *Fractional crystallization*

Mafic dikes from the Xinfangzi and Shangxigou areas analysed during this study have high $Mg^{\#}$ values (48–60; Table 2), inconsistent with significant crystal fractionation. However, the fact that MgO concentrations negatively correlate with SiO_2, TiO_2, Fe_2O_3, and P_2O_5 in all samples analysed during this study (Figures 5A, 5B, 5D, and 5H) suggests that the magmas that formed these mafic dikes were derived from fractionation of olivine, pyroxene, and Ti-bearing phases (rutile, ilmenite, titanite, etc.) from a more mafic parental magma. The separation of plagioclase could also account for the observed negative Eu anomalies in chondrite-normalized REE patterns (Figure 6A), and the relationships between Eu_N/Eu^* values and Sr and Rb concentrations (plots not shown) indicate that the dolerites underwent both K-feldspar and plagioclase fractionation.

5.4 *Genetic processes and model of formation*

All samples analysed during this study plot along a partial melting trend (positive correlation) on La *versus* La/Sm diagrams (not shown), indicating that the mafic dikes formed from magmas derived from partial melting of a region of the asthenospheric mantle. However, chondrite-normalized REE diagrams indicate that dikes from the two study areas either formed from differing sources or have significantly differing igneous histories; for example, XFZ1-13 dike samples are strongly LREE-enriched and HREE-depleted, suggesting they were derived from magmas formed during partial melting of a region of the mantle that contained residual garnet, whereas the REE characteristics of the SXG1-9 dikes do not indicate sourcing from a region of the mantle that contained residual garnet.

The data presented here suggest that mafic dikes in the study area formed from magmas derived from partial melting of a region of the asthenospheric mantle, with differences between the two dike suites relating to garnet-present or garnet-absent melting. However, a dynamic model is required to further decipher the origin of these rocks. The timing and direction of collisional tectonics in the NCC (Engebretson *et al.* 1985; Xu *et al.* 1993; Shen *et al.* 1994; Zhang *et al.* 1995; Yuan 1996; Meng and Zhang 1999; Zhang *et al.* 2001; Hu *et al.* 2004; Liu *et al.* 2005; Zhang *et al.* 2005) means that the subducting Yangtze lithosphere and the ancient Pacific Plate did not contribute to the source of the magmas that formed these dikes. Here, we present an

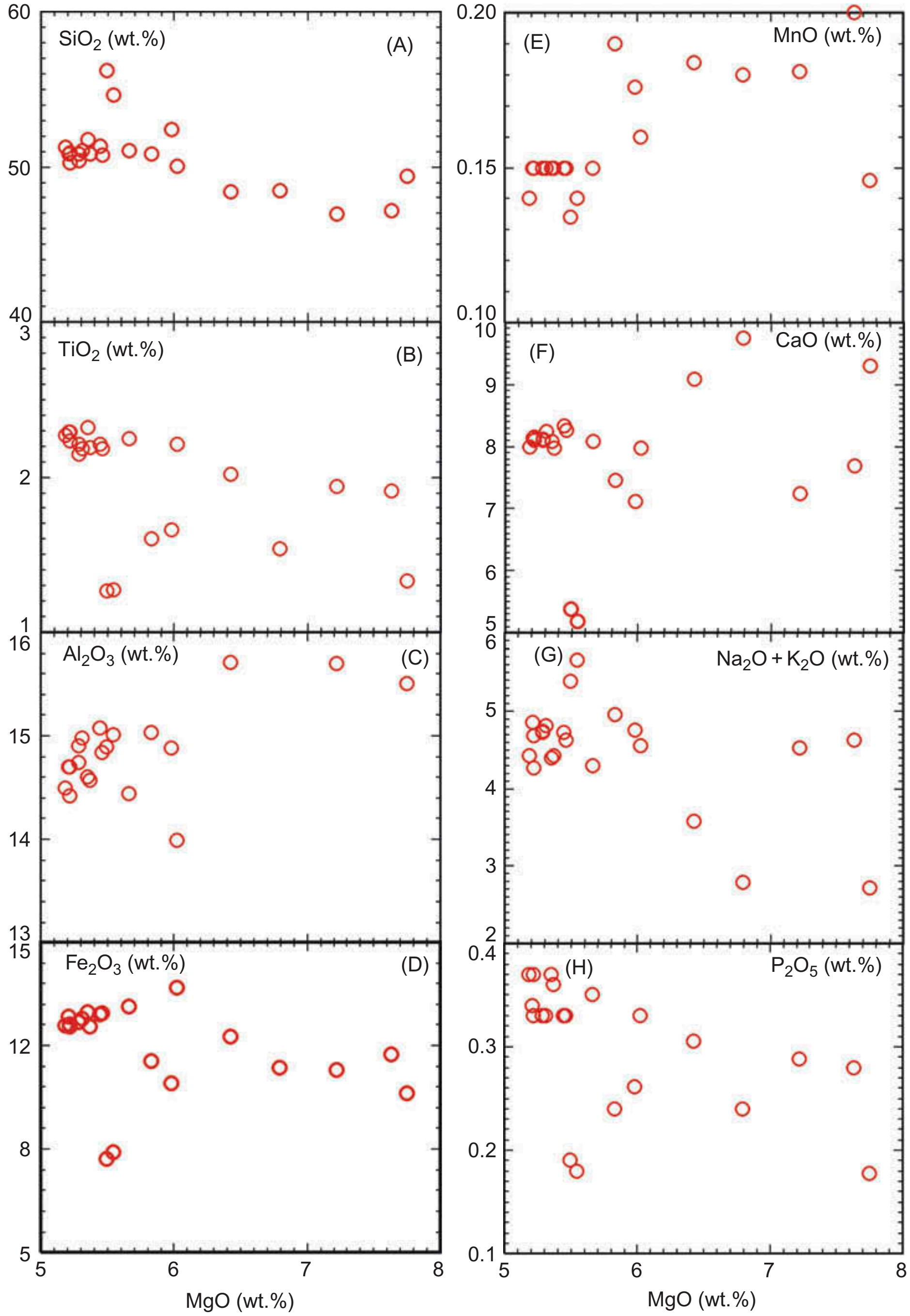

Figure 5. Variations in major element concentrations compared with MgO (in wt.%) for mafic dikes of the northern NCC, China.

alternative model that accounts for the origin of these mafic dikes.

The study areas are within the northern part of the NCC, to the south of the Siberian Block. The timing of collision between these blocks is controversial (Miyashiro 1981; Tang 1990; Shao 1991; Wang *et al.* 1991; Hong *et al.* 1994; Zhang *et al.* 2007; Miao *et al.* 2008; Zhang *et al.* 2008; Luo *et al.* 2009; Chen *et al.* 2012), although there is increasing evidence for a pre-early Permian (i.e. Palaeozoic) collision (e.g. Miyashiro 1981; Zhang *et al.* 2008; Zhou *et al.* 2010). After collision, the study areas underwent relaxation and extension, which led to crustal thinning and decompression partial melting of a region of the asthenospheric mantle that ultimately resulted in the emplacement of mafic dike swarms.

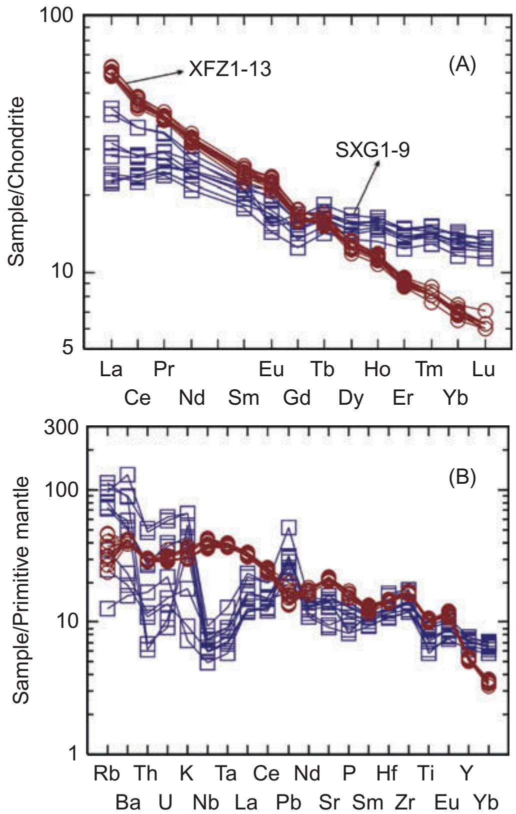

Figure 6. (A) Chondrite-normalized REE and (B) primitive mantle-normalized incompatible element distribution diagrams for mafic dikes of the northern NCC, China; concentrations are normalized to the chondrite and primitive mantle values of Sun and McDonough (1989).

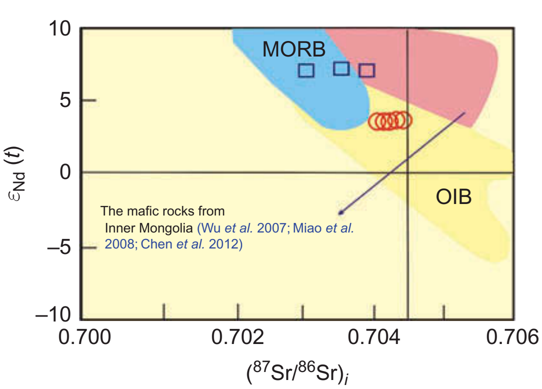

Figure 7. Diagram showing variations in initial $^{87}Sr/^{86}Sr$ *versus* $\varepsilon_{Nd}(t)$ values for mafic dikes of the northern NCC, China. Also shown is a field delineating the composition of Palaeozoic mafic rocks within the NCC (Wu *et al.* 2007; Miao *et al.* 2008; Chen *et al.* 2012). The NCC mafic dikes analysed during this study plot within the depleted mantle source field.

We therefore propose the following genetic model that accounts for the presence of mafic dikes in the northern NCC: (a) Prior to collision, the NCC and the Siberian Block were two independent crustal blocks. (b) Collision

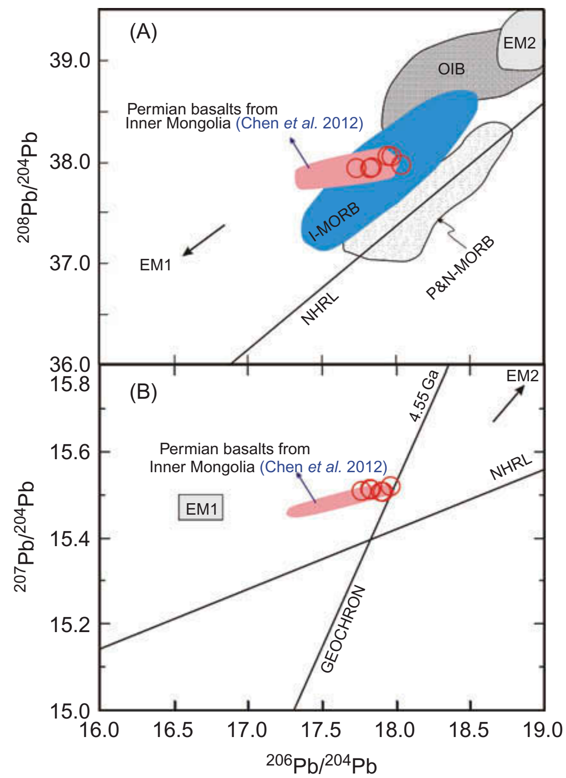

Figure 8. Relationship between $^{208}Pb/^{204}Pb$ and $^{207}Pb/^{204}Pb$ *versus* $^{206}Pb/^{204}Pb$ values for alkaline felsic rocks compared with Permian basalts from Inner Mongolia (Chen *et al.* 2012). The fields for Indian, Pacific, and North Atlantic MORB, OIB, and NHRL are from Zou *et al.* (2000), and the 4.55 Ga geochron is from Hart (1984).

between the NCC and the Siberian Block occurred before the Permian, with crustal shortening and collision causing thickening of the lithospheric mantle beneath both regions. This thickened lithosphere was associated with deformation and regional metamorphism, coincident with the transformation of supracrustal rocks that led to the formation of ophiolites within the collisional zone. (c) Density differences in this mélange caused gravitational instabilities, leading to the foundering of denser crustal units into the asthenosphere. The terminal stage of collision between the two crustal blocks was followed by relaxation and lithospheric extension, leading to buoyant upwelling of hot asthenospheric material that locally increased geothermal gradients, causing partial melting of ultramafic lithologies within both asthenospheric and lithospheric mantle regions beneath the NCC and Siberian crustal blocks. These partial melts, which were the mafic parental magmas for the mafic dikes discussed here, underwent fractionation but did not assimilate any crustal material prior to or during ascent and emplacement. These magmas also formed other igneous rocks within the NCC (e.g. Permian basalts in Inner Mongolia; Figures 7 and 8).

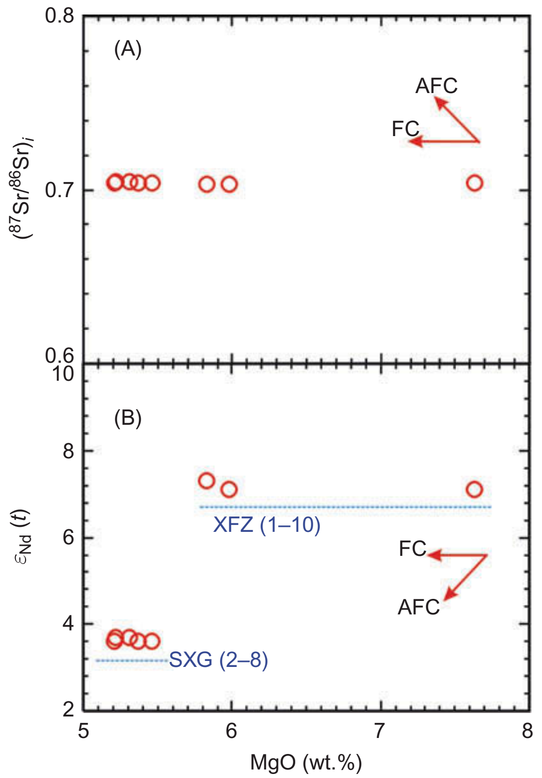

Figure 9. Variations in (A) initial $^{87}Sr/^{86}Sr$ ratios and (B) ε_{Nd} (t) values with changing MgO concentrations for mafic dikes of the northern NCC, China.

6. Conclusions

Based on geochronological, geochemical, and Sr–Nd–Pb isotopic data presented here, we reach the following conclusions:

(1) U–Pb dating of zircons indicates that mafic dikes within Hebei Province and Inner Mongolia formed between 275.0 ± 4.5 and 274.82 ± 2.9 Ma, indicating Permian magmatism.

(2) The dolerites examined in this study crystallized from magmas derived from a depleted asthenospheric mantle. The parental magmas of these dike swarms underwent fractionation during ascent and/or emplacement, precipitating olivine, pyroxene, plagioclase, K-feldspar, and Ti-bearing phases (rutile, ilmenite, and titanite), with negligible crustal contamination.

(3) The generation and emplacement of these magmas was associated with post-collisional relaxation that promoted upwelling of the asthenospheric mantle. This rising mantle underwent decompression partial melting, yielding the mafic parental melts of the dikes. Extensional tectonics also facilitated crustal thinning and possibly rifting, providing easy pathways for the migration and emplacement of the evolved dolerite dike swarms.

Acknowledgements

This research was supported by the Knowledge Innovation Project (KZCX2-YW-111-03) and the Opening Project (08LCD08) of the State Key Laboratory of Continental Dynamics. The authors gratefully acknowledge Lian Zhou for assistance with Sr–Nd–Pb isotope analysis and Zhaochu Hu for assistance with LA-ICP-MS zircon U–Pb dating.

References

Andersen, T., 2002, Correction of common lead in U-Pb analyses that do not report ^{204}Pb: Chemical Geology, v. 192, p. 59–79.

Chen, C., Zhang, Z.C., Guo, Z.J., Li, J.F., Feng, Z.X., and Tang, W.H., 2012, The geochronology, geochemistry and geological significance of the early Permian mafic rocks in Damaoqi Mandula, Inner Mongolia: Sciences in China, v. 42, p. 343–358.

Chen, X.D., and Shi, L.B., 1983, Primary research on the diabase dyke swarms in Wutai–Taihang area: Chinese Science Bulletin, v. 16, p. 1002–1005.

Chen, X.D., and Shi, L.B., 1994, Basic dyke swarms in extensional structures, *in* Qian, X.L., ed., Extensional structures: Beijing, Geological Publishing House, p. 71–74.

Chen, X.D., Shi, L.B., and Jia, S.F., 1992, Proterozoic basic dyke swarms in North China: Seismology and Geology, v. 14, p. 351–357 (in Chinese with English abstract).

Engebretson, D.C., Cox, A.V., and Gordon, R.G., 1985, Relative motions between oceanic and continental plates in the Pacific basin: Geological Society of America Special Paper, v. 206, 59 p.

Gao, S., Luo, T.-C., Zhang, B.-R., Zhang, H.-F., Han, Y.-W., Zhao, Z.-D., and Hu, Y.-K., 1998a. Chemical composition of the continental crust as revealed by studies in East China: Geochimica et Cosmochimica Acta, v. 62, p. 1959–1975.

Gao, S., Zhang, B.-R., Jin, Z.-M., Kern, H., Luo, T.-C., and Zhao, Z.-D., 1998b, How mafic is the lower continental crust?: Earth and Planetary Science Letters, v. 106, p. 101–117.

Hall, H.C., 1982, The importance and potential of mafic dyke swarms in studies of geodynamic process: Geosciences Canada, v. 9, p. 145–154.

Hall, H.C., and Fahrig, W.F., 1987, Mafic dyke swarms: Geological Association of Canada Special Paper, v. 34, p. 1–503.

Hart, S.R., 1984, A large-scale isotope anomaly in the Southern Hemisphere mantle: Nature, v. 309, p. 753–757.

Hirajima, T., Ishiwatari, A., Cong, B., Zhang, R., Banno, S., and Nozaka, T., 1990, Coesite from Mengzhong eclogite at Donghai county, northern Jiangsu province, China: Mineralogy Magazine, v. 54, p. 579–583.

Hong, D.W., Huang, H.Z., Xiao, Y.J., Xu, H.M., and Jin, M.Y., 1994, The Permian alkaline granites in central Inner Mongolia and their geodynamic significance: Acta Geologica Sinica, v. 68, p. 219–230 (in Chinese with English abstract).

Hou, G.T., Liu, Y.L., and Li, J.H., 2006, Evidence for 1.8 Ga extension of the Eastern Block of the North China Craton from SHRIMP U–Pb dating of mafic dyke swarms in Shandong Province: Journal of Asian Earth Sciences, v. 27, p. 392–401.

Hu, J.M., Zhao, G.C., Ma, G.L., Zhang, S.Q., and Gao, D.S., 2004, Paleozoic exensional tectonics of the Wudang block in the Qinling Orogen, China: Chinese Journal of Geology, v. 39, p. 305–319 (in Chinese with English abstract).

Hu, R.Z., Bi, X.W., and Zhou, M.F., 2008, Uranium metallogenesis in South China and its relationship to crustal extension during the Cretaceous to Tertiary: Economic Geology, v. 103, p. 583–598.

John, D.A.P., Zhang, J.S., Huang, B.C., and Andrew, P.R., 2010, Palaeomagnetism of Precambrian dyke swarms in the North China Shield: The 1.8 Ga LIP event and crustal consolidation in late Palaeoproterozoic times: Journal of Asian Earth Sciences, v. 41, p. 504–524.

Kato, T., Enami, A., and Zhai, M., 1997, Ultrahigh-pressure marble and eclogite in the Su-Lu ultrahigh-pressure terrane, eastern China: Journal of Metamorphic Geology, v. 15, p. 169–182.

Le Maitre, R.W., 2002, Igneous rocks: A classification and glossary of terms (second edition): Cambridge, Cambridge University Press, p. 236.

Li, T.S., Zhai, M.G., Peng, P., Chen, L., and Guo, J.H., 2010, Ca. 2.5 billion year old coeval ultramafic-mafic and syenitic dykes in Eastern Hebei: Implications for cratonization of the North China Craton: Precambrian Research, v. 180, p. 143–155.

Liu, S., Hu, R., Gao, S., Feng, C., Coulson, I.M., Feng, G., Qi, Y., Yang, Y., Yang, C., and Tang, L., 2012a, U-Pb zircon age, geochemical and Sr-Nd isotopic data as constraints on the petrogenesis and emplacement time of the Precambrian mafic dyke swarms in the North China Craton (NCC): Lithos, v. 140–141, p. 38–52. doi: 10.1016/j.lithos.2012.01.002.

Liu, S., Hu, R., Gao, S., Feng, C., Coulson, I.M., Feng, G., Qi, Y., Yang, Y., Yang, C., and Tang, L., 2013, Zircon U-Pb age and Sr-Nd-Hf isotopic constraints on the age and origin of Triassic mafic dikes, Dalian area, Northeast China: International Geology Review, v. 55, p. 249–262. doi: 10.1080/00206814.2012.707003.

Liu, S., Hu, R., Gao, S., Feng, C., Feng, G., Qi, Y., Coulson, I.M., Yang, Y., Yang, C., and Tang, L., 2012b, Geochemical and isotopic constraints on the age and origin of mafic dikes from eastern Shandong Province, eastern North China Craton: International Geology Review, v. 54, p. 1389–1400. doi: 10.1080/00206814.2011.641732.

Liu, S., Hu, R., Gao, S., Feng, C., Qi, Y., Wang, T., Feng, G., and Coulson, I.M., 2008a, U-Pb zircon age, geochemical and Sr-Nd-Pb-Hf isotopic constraints on age and origin of alkaline intrusions and associated mafic dikes from Sulu orogenic belt, Eastern China: Lithos, v. 106, p. 365–379. doi: 10.1016/j.lithos.2008.09.004.

Liu, S., Hu, R., Gao, S., Feng, C., Yu, B., Feng, G., Qi, Y., Wang, T., and Coulson, I.M., 2009, Petrogenesis of Late Mesozoic mafic dykes in the Jiaodong Peninsula, eastern North China Craton and implications for the foundering of lower crust: Lithos, v. 113, p. 621–639. doi: 10.1016/j.lithos.2009.06.035.

Liu, S., Hu, R.-Z., Gao, S., Feng, C.-X., Qi, L., Zhong, H., Xiao, T., Qi, Y.-Q., Wang, T., and Coulson, I.M., 2008b, Zircon U-Pb geochronology and major, trace elemental and Sr-Nd-Pb isotopic geochemistry of mafic dykes in western Shandong Province, east China: Constrains on their petrogenesis and geodynamic significance: Chemical Geology, v. 255, p. 329–345. doi: 10.1016/j.chemgeo.2008.07.006.

Liu, S., Hu, R.Z., Zhao, J.H., Feng, C.X., Zhong, H., Cao, J.J., and Shi, D.N., 2005, Geochemical characteristics and petrogenetic investigation of the late Mesozoic lamprophyres of Jiaobei, Shandong Province: Acta Petrologica Sinica, v. 21, p. 947–958 (in Chinese with English abstract).

Liu, S., Zou, H.B., Hu, R.Z., Zhao, J.H., and Feng, C.X., 2006, Mesozoic mafic dikes from the Shandong Peninsula, North China Craton: Petrogenesis and tectonic implications: Geochemical Journal, v. 40, p. 181–195.

Liu, Y.S., Hu, Z.C., Zong, K.Q., Gao, C.G., Gao, S., Xu, J., and Chen, H.H., 2010, Reappraisement and refinement of zircon U-Pb isotope and trace element analyses by LA-ICP-MS: Chinese Science Bulletin, v. 55, p. 1535–1546.

Ludwig, K.R., 2003, User's manual for Isoplot/Ex, Version 3.00. A geochronological toolkit for Microsoft Excel: Berkeley Geochronology Center Special Publication, v. 4, p. 1–70.

Lugmair, G.W., and Harti, K., 1978, Lunar initial 143Nd/144Nd: Differential evolution of the lunar crust and mantle: Earth and Planetary Science Letters, v. 39, p. 349–357.

Luo, H.L., Wu, T.R., and Zhao, L., 2009, Permian high Ba-Sr granitoids: Geochemistry, age and tectonic implications of Erlangshan pluton, Urad Zhongqi, Inner Mongolia: Acta Geological Sinica, v. 83, p. 603–614.

Meng, Q., and Zhang, G., 1999, Timing of collision of the North and South China blocks: Controversy and reconciliation: Geology, v. 27, p. 123–126.

Miao, L.C., Fan, W.M., and Liu, D.Y., 2008, Geochronology and geochemistry of the Hegenshan phiolitic complex: Implications for late-stage tectonic evolution of the Inner Mongolia-Daxinganling Orogenic Belt, China: Journal of Asian Earth Sciences, v. 32, p. 348–370.

Middlemost, E.A.K., 1994, Naming materials in the magma/igneous rock system: Earth-Science Reviews, v. 74, p. 193–227.

Miyashiro, A., 1981, Tectonic and petrologic aspects of Asia: Memoir. Geological Society of China, Taipei, v. 4, p. 1–31.

Peng, P., 2010, Reconstruction and interpretation of giant mafic dyke swarms: A case study of 1.78 Ga magmatism in the North China craton: Geological Society Special Publication 338: London, Geological Society, p. 163–178.

Peng, P., Bleeker, W., Ernst, R.E., Söderlund, U., and McNicoll, V., 2011a, U–Pb baddeleyite ages, distribution and geochemistry of 925 Ma mafic dykes and 900 Ma sills in the North China craton: Evidence for a Neoproterozoic mantle plume: Lithos, v. 127, p. 210–221.

Peng, P., Guo, J.H., Zhai, M.G., and Bleeker, W., 2010, Paleoproterozoic gabbronoritic and granitic magmatism in the northern margin of the North China craton: Evidence of crust–mantle interaction: Precambrian Research, v. 183, p. 635–659.

Peng, P., Zhai, M.G., Guo, J.H., Kusky, T., and Zhao, T.P., 2007, Nature of mantle source contributions and crystal differentiation in the petrogenesis of the 1.78 Ga mafic dykes in the central North China craton: Gondwana Research, v. 12, p. 29–46.

Peng, P., Zhai, M.G., Li, Q.L., Wu, F.Y., Hou, Q.L., Li, Z., Li, T.S., and Zhang, Y.B., 2011b, Neoproterozoic (900 Ma) Sariwon sills in North Korea: Geochronology, geochemistry and implications for the evolution of the south-easternmargin of the North China Craton: Gondwana Research, v. 20, p. 243–254.

Peng, P., Zhai, M.-G., Li, Z., Wu, F.-Y., and Hou, Q.-L., 2008, Neoproterozoic (∼820 Ma) mafic dyke swarms in the North China craton: Implication for a conjoint to the Rodinia supercontinent? *In* Abstracts, 13th Gondwana Conference: Dali, p. 160–161.

Peng, P., Zhai, M.-G., Zhang, H.-F., and Guo, J.-H., 2005, Geochronological constraints on the Palaeoproterozoic evolution of the North China Craton: SHRIMP zircon ages of different types of mafic dikes: International Geology Review, v. 47, p. 492–508.

Potts, P.J., and Kane, J.S., 2005, International association of geoanalysts certificate of analysis: Certified reference material

OU-6 (Penrhyn slate): Geostandards and Geoanalytical Research, v. 29, p. 233–236.
Qi, L., Hu, J., and Grégoire, D.C., 2000, Determination of trace elements in granites by inductively coupled plasma mass spectrometry: Talanta, v. 51, p. 507–513.
Saunders, A.D., Storey, M., Kent, R.W., and Norry, M.J., 1992, Consequences of plume-Lithosphere interactions, *in* Storey, B.C., Alabaster, T., and Pankhurst, R.J., eds., Magmatism and the cause of continental breakup: Geological Society, London Special Publication, v. 68, p. 41–60.
Shao, J.A., 1991, Middle crust evolution in north margin of Sino-Korea plate: Beijing, Peking University Press, p. 136 (in Chinese).
Shao, J.A., and Zhang, L.Q., 2002, Mesozoic dyke swarms in the north of North China: Acta Petrologica Sinica, v. 18, p. 312–318.
Shao, J.A., Zhang, Y.B., Zhang, L.Q., Mu, B.L., Wang, P.Y., and Guo, F., 2003, Early Mesozoic dyke swarms of carbonatites and lamprophyres in Datong area: Acta Petrologica Sinica, v. 19, p. 93–104.
Shen, H.C., Kang, W.G., and Liang, W.T., 1994, A discussion about the collision time between Northern China plate and Yangzi plate: Journal of Changchun University of Earth Sciences, v. 24, p. 22–27 (in Chinese with English abstract).
Steiger, R.H., and Jäger, E., 1977, Subcommission on geochronology; convention on the use of decay constants in geochronology and cosmochronology: Earth and Planetary Science Letters, v. 36, p. 359–362.
Sun, S.S., and McDonough, W.F., 1989, Chemical and isotopic systematics of oceanic basalts: Implications for mantle composition and processes, *in* Saunders, A.D., and Norry, M.J., eds., Magmatism in the Ocean Basins: London, Geological Society Special Publication, p. 313–345.
Tang, K.D., 1990, Tectonic development of Paleozoic foldbelts at the northern margin of the Sino-Korean Craton: Tectonics, v. 9, p. 249–260.
Tarney, J., and Weaver, B.L., 1987, Geochemistry and petrogenesis of early Proterozoic dyke swarms, *in* Halls, H.C., and Fahrig, W.C., eds., Mafic dyke swarms: Special Publication-Geological Association of Canada, v. 34, p. 81–93.
Thompson, M., Potts, P.J., Kane, J.S., and Wilson, S., 2000, An international proficiency test for analytical geochemistry laboratories-report on round 5 (August 1999). Geostandards and Geoanalytical Research, v. 24, p. E1–E28.
Wang, Q., Liu, X.Y., and Li, J.T., 1991, Plate tectonics between Cathaysia and Angaraland: Peking, Peking University Press, p. 151 (in Chinese with English abstract).
Wang, T., Zheng, Y.D., Zhang, J.J., Wang, X.S., Zeng, L.S., and Tong, Y., 2007, Some problems in the study of Mesozoic extensional structure in the North China Craton and its significance for the study of lithospheric thinning: Geological Bulletin of China, v. 26, p. 1154–1166 (in Chinese with English abstract).
Wang, Y.M., Gao, Y.S., Han, H.M., and Wang, X.H., 2003, Practical handbook of reference materials for geoanalysis: Geological Publishing House (in Chinese).
Wu, F.Y., Xu, Y.G., Gao, S., and Zheng, J.P., 2008, Lithospheric thinning and destruction of the North China Craton: Acta Petrologica Sinica, v. 24, p. 1145–1174 (in Chinese with English abstract).
Wu, F.Y., Zhao, G.C., and Sun, D.Y., 2007, The hulan group: Its role in the evolution of the central Asian orogenic belt of NE China: Journal of Asian Earth Sciences, v. 30, p. 542–556.
Xu, J.W., Ma, G.F., Tong, W.X., Zhu, G., and Lin, S.F., 1993, Displacement of Tancheng-Lujiang Wrench fault system and its geodynamic setting in the northwestern Circum-pacific, *in* Xu, J., ed., The Tanch eng-Lujiang Wrench system: New York, John Wiley & Sons, p. 51–74.
Xu, Y.G., 2004, Lithospheric thinning beneath North China: A temporal and spatial perspective: Geological Journal of China Universities, v. 10, p. 324–331 (in Chinese with English abstract).
Yang, J.H., Chung, S.L., Zhai, M.G., and Zhou, X.H., 2004, Geochemical and Sr–Nd–Pb isotopic compositions of mafic dikes from the Jiaodong Peninsula, China: Evidence for vein-plus-peridotite melting in the lithospheric mantle: Lithos, v. 73, p. 156–160.
Yuan, H.L., Gao, S., Liu, X.M., Li, H.M., Gunther, D., and Wu, F.Y., 2004, Accurate U-Pb age and trace element determinations of zircon by laser ablation-inductively coupled plasma mass spectrometry: Geostandards Newsletter, v. 28, p. 353–370.
Yuan, X.C., 1996, Altas of geophysics in China, *in* Yuan, X.C., ed., Geophysical map collections in China: Beijing, Geological Press, p. 59–62 (in Chinese with English abstract).
Zhai, M.G., Fang, H.R., Yang, J.H., and Miao, L.C., 2004, Large-scale cluster of cold deposits in east Shandong: Anorogenic metallogenesis: Earth Science Frontiers, v. 11, p. 95–98 (in Chinese with English abstract).
Zhai, M.G., Zhu, R.X., Liu, J.M., Meng, Q.R., Hou, Q.L., Hu, S.B., Li, Z., Zhang, H.F., and Liu, W., 2003, The critical time frame of turning pint of tectonic regime: Sciences in China (D), v. 33, p. 913–920.
Zhang, C.H., 2009, Selected tectonic topics in the investigation of geodynamic process of destruction of North China Craton: Earth Science Frontiers, v. 16, p. 203–214 (in Chinese with English abstract).
Zhang, G.W., Meng, Q.R., and Lai, S.C., 1995, Tectonics and structure of Qinling orogenic belt: Science in China, Series B, v. 38, p. 1379–1394.
Zhang, H.F., and Sun, M., 2002, Geochemistry of Mesozoic basalts and mafic dikes, southeastern north China Carton, and tectonic implications: International Geology Review, v. 44, p. 370–382.
Zhang, H.F., Sun, M., Zhou, X.H., and Ying, J.F., 2005, Geochemical constraints on the origin of Mesozoic alkaline intrusive complexes from the North China Craton and tectonic implications: Lithos, v. 81, p. 297–317.
Zhang, Q., Zhao, T.P., Wang, Y., and Wang, Y.L., 2001, A discussion on the Yanshanian magmatism in eastern China: Acta Petrologica et Mineralogica, v. 20, p. 273–280 (in Chinese with English abstract).
Zhang, S.H., Zhao, Y., and Song, B., 2007, Carboniferous granitic plutons from the northern margin of the North China block: Implications for a late Paleozoic active continental margin: Journal of the Geological Society of London, v. 164, p. 451–463.
Zhang, X.H., Zhang, H.F., and Tang, Y.J., 2008, Geochemistry of Permian bimodal volcanic rocks from central Inner Mongolia, North China: Implication for tectonic setting and Phanerozoic continental growth in Central Asian Orogenic Belt: Chemical Geology, v. 249, p. 262–281.
Zhao, G.C., Wilde, S.A., Cawood, P.A., and Sun, M., 2001, Archean blocks and their boundaries in the North China Craton: Lithological, geochemical, structural and P-T path constraints and tectonic evolution: Precambrian Research, v. 107, p. 45–73.

Zhao, J.X., and McCulloch, M.T., 1993, Melting of a subduction-modified continental lithosphericmantle: Evidence from late Proterozoic mafic dike swarms in central Australia: Geology, v. 21, p. 463–466.

Zhou, Z.G., Gu, Y.C., Liu, C.F., Yu, Y.S., Zhang, B., Tian, Z.J., He, F.B., and Wang, B.R., 2010, Discovery of Early-Middle Permian cathaysian flora in Manduhubaolage area, Dong Ujimqin Qi, Inner Mongolia, China and its geological significance: Geological Bulletin of China, v. 29, p. 21–25 (in Chinese with English abstract).

Zhu, G., Hu, Z.Q., Chen, Y., Niu, M.L., and Xie, C.L., 2008, Evolution of Early Cretaceous extensional basins in the eastern North China craton and its destruction of the craton: Geological Bulletin of China, v. 27, p. 1594–1604 (in Chinese with English abstract).

Zou, H.B., Zindler, A., Xu, X.S., and Qi, Q., 2000, Major, trace element, and Nd, Sr and Pb isotope studies of Cenozoic basalts in SE China: Mantle sources, regional variations and tectonic significance: Chemical Geology, v. 171, p. 33–47.